Northward IMF plasma sheet entropies

Jay R. Johnson[1] and Simon Wing[2]

[1]Princeton Plasma Physics Laboratory, Princeton, New Jersey, USA

[2]The Johns Hopkins University Applied Physics Laboratory, Laurel, Maryland, USA

Abstract. The plasma sheet pressure, temperature, and density profiles inferred from DMSP observations are used to investigate northward IMF plasma sheet specific entropy, $s = p/\rho^{\gamma}$ or p/n^{γ} (for a single ion species). The specific entropy is approximately conserved in the X or convection direction, but it also has a gradient in the Y-direction. The hot ion population entropy profile suggests a dawn to dusk azimuthal heat flux that is consistent with the curvature and gradient drift. In contrast, the entropy of the cold population is approximately conserved in the X direction but has a strong gradient toward the midnight meridian. The cold population entropy is higher than that of the magnetosheath, suggesting the entry process may heat the ions. Cusp reconnection by itself may not increase the magnetosheath ion entropy, but cusp reconnection with kinetic Alfvén waves (KAW) may provide the necessary heating. Localized reconnection in Kelvin-Helmholtz vortices may increase the entropy if the plasma expands nonadiabatically into the large magnetospheric flux tube volume. KAWs may lead to diffusion and heating consistent with the observations. Entropy increases by a factor of five from the flanks to the midnight meridian, which provides a constraint for transport mechanism(s) within the plasma sheet. A simple calculation is performed to demonstrate that the spatial gradients of entropy in the plasma sheet could result from the temporal dependence of transport processes in the magnetopause boundary layer.

1. Introduction

Satellite observations show that the Earth's plasma sheet ions become cold and dense during periods of northward interplanetary magnetic field (IMF), which has been attributed to the massive transport of solar wind or magnetosheath ions into the plasma sheet [e.g., *Terasawa et al*., 1997; *Fujimoto et al*., 1998; Wing et al., 2002; 2005;2006]. Recently, Wing et al. [2007] studied an event in which the interplanetary magnetic field (IMF) was northward for almost one day. The plasma sheet dawn and dusk flanks appeared to reach cold dense states ($n > 1$ cm^{-3}; $T < 2$ keV) within a few hours after IMF northward turning. Closer to the center (midnight meridian), the ion temperatures reach < 2 keV within a few hours of IMF northward turning, but the ion densities never reached above 1 cm^{-3} for at least ~8 hours after IMF northward turning.

Several solar wind entry mechanisms into the plasma sheet have been proposed. The leading mechanisms include poleward of the cusp reconnection in both hemispheres [e.g., *Song and Russell*, 1992] and diffusive processes, e.g., Kelvin-Helmholtz instability (KHI) [e.g., *Otto and Fairfield*, 2000] and kinetic Alfvén waves (KAW) [e.g., *Johnson and Cheng*, 1997]. Presently, it is not clear which of these mechanisms is dominant. Wing et al. [2007] estimated the plasma sheet filling rates for cusp entry and diffusive processes and found that theoretical filling rates were comparable and consistent with the observed filling rates that were observed both in situ by GEOTAIL and remotely by DMSP [Wing et al., 2007]. The result suggests that all three mechanisms can play significant roles in filling the plasma sheet and (2) plasma sheet filling rate may not be able to distinguish these three mechanisms (although cusp entry and diffusive entry do scale differently with the solar wind/magnetosheath density). However, in addition to the timescale for the formation of CDPS there are additional constraints such as dawn-dusk asymmetries and entropy conservation that provide additional observational constraints for these various entry mechanisms.

In the study of the transport of plasma into and within plasma sheet, it is often useful to consider what parameters are conserved and under what conditions. Conserved quantities are particularly useful to help simplify modeling of a system. Conversely, breaking of conservational invariants may be an indicator that a more complicated model is required. One fundamental conserved quantity is the entropy, which is conserved when the plasma response is adiabatic. In the ideal MHD description, the pressure response is generally prescribed as adiabatic such that the entropy per unit mass (also referred to as specific entropy), $s= p/\rho^{\gamma}$, is constant for a fluid element where p = the plasma pressure, B = magnetic field, γ = the polytropic index. The specific entropy, s, should be rigorously conserved in an ideal MHD fluid element and is an intensive variable in that it does not depend on system size. The pressure equation also implies an integral constraint on the total mass content of a flux tube, $M = \int\rho\ ds/B$ and total content of a flux tube, $N = \int n\ ds/B$ (for single ion species) are proportional to $S= \int p^{1/\gamma}\ ds/B$. Although not precisely the entropy of the flux tube, this quantity S is entropy-like in nature [*Birn et al*., 2006] and we will refer to it as the total entropy. The total entropy is also an important parameter to identify when the interchange instability is operable.

Nonconservation of specific entropy is expected to occur when nonadiabatic processes such as wave-particle interactions, heat flux, and dissipation are operating and when the fluid element looses its integrity as occurs when hot particles and cold particles move differently (e.g. cold particles move with ExB convection and hot particles move by curvature and gradient drift). Nonconservation of specific entropy is normally an indicator that an MHD description is inadequate and kinetic or dissipative processes should be included in the dynamical evolution of the system.

In the case of a single ion species, $p/\rho^{\gamma} \sim p/n^{\gamma}$. If s is conserved along the convection path, then, in the p – n space, plasma sheet ion p and n should follow lines having constant slopes of γ, termed adiabats. Borovsky et al. [1998] shows that statistically this seems to be the case from midtail region (X = -22.5 Re) to geosynchronous orbit (X = - 6.6 Re) in their p – n plots (see their Plate 1). Borovsky et al. [1998] finds that $\gamma = 1.52$, which is close to 5/3, albeit the scatters are quite large. Similar result has been obtained by Baumjohann [1993] that reports that $\gamma \sim 1.69$ also with large scatters in its p – n plots.

Where s is conserved, it should be expected that contours of constant s are related to drift paths. However, in the case of energy dependent drifts such as the curvature and gradient drifts, the fluid element can be compromised where cold particles move with ExB and hot particles move according to curvature and gradient drift. However, it is still possible to consider conservation of entropy for particles in a given energy range, which would be conserved along their drift paths.

Nonconservation of the total entropy can also occur where nonadiabatic processes are operating, but because it is an integral constraint for a particular flux tube, a localized process that changes the specific entropy in a small region of the flux tube may not significantly affect the total entropy so that changes in S may not indicate significant changes in s. However, if the localized process leads to field-line reconfiguration (reconnection), then the change of entropy is more related to the change of flux tube volume than to changes in specific entropy in that volume. In this way, reconnection processes can significantly affect total entropy while introducing little change in the specific entropy as shown theoretically and observationally for substorms [Birn et al., 2004,2006; Wing et al., 2007, 2008].

For purposes of this study, we will be considering the entropy of plasma in the plasma sheet for northward IMF configuration. Because the plasma sheet electron contribution to the

total pressure is much smaller, roughly 15% [e.g., Baumjohann et al., 1989; Spence et al., 1989], than the ion pressure, it is possible to probe the plasma sheet entropy considering only ion data. In the plasma sheet, ions have been observed to be nearly isotropic irrespective of magnetic activities [Kistler et al., 1992; Huang and Frank, 1994; Spence et al., 1989] due to strong (elastic) pitch angle scattering [e.g., Lyons and Speiser, 1982] and long drift time compared to the bounce period [e.g., Wolf, 1983]. Fortunately, the isotropy of the ions makes it possible to remotely probe the ion distributions by observing only precipitating particles in the ionosphere as discussed later. Moreover, because the pressure is observed to be isotropic, the total entropy can be simplified when the system is near equilibrium because the pressure is constant along field lines and $S \sim p^{1/\gamma}V$ (V is flux tube volume) is conserved. Interestingly, Usadi et al. [2006] notes that even when the particle motion violates both first and second adiabatic invariant, S is still conserved. The value for γ can range from 0 to ∞, depending on the process(es) involved. For example, for isobaric (constant pressure) system, $\gamma = 0$, for isothermal (constant temperature) system $\gamma = 1$, for isometric (constant density) system $\gamma = \infty$, and for adiabatic (no heat loss) system and monoatomic gas $\gamma = 5/3$. $S = p^{1/\gamma}V$ is an extensive parameter that is proportional to system size, e.g., flux tube volume V.

The present study will focus primarily on the specific entropy profiles in the plasma sheet under northward IMF configuration. In particular, we will consider the entropy of all the observed plasma as well as the entropy of plasma measured in two energy ranges corresponding to cold, dense plasma and nominal hot plasma sheet material. Our investigation will show that the entropy profiles are significantly different for these two energy ranges indicating that the two populations evolve according to different dynamics. We will also investigate the conservation of these entropies and discuss the relevance of entropy nonconservation to plasma entry processes.

2. Dataset

This study used data from the SSJ4 instrument on board Defense Meteorological Satellite Program (DMSP) satellites F8, F9, F10, and F11 for the entire year of 1992. In 1992, there were at least three DMSP satellites in operation simultaneously (F8, F10, and either F9 or F11) and for one month, March, all four were in operation. Because 1992 is near solar maximum, this choice of dataset introduces some biases to those plasma sheet parameters that have solar cycle dependences. For example, the average solar wind density is well correlated with the average plasma sheet density; hence both values should be higher near solar maximum [*Borovsky et al*., 1998; *Papitashvili et al*., 2000].

The SSJ4 instrumental package included on all recent DMSP flights uses curved figure electrostatic analyzers to measure ions and electrons from 32 eV to 30 keV in logarithmically spaced steps [*Hardy et al*., 1984]. Because of its upward pointing and limited pitch-angle resolution, DMSP SSJ4 measures only highly field-aligned precipitating particles at an altitude of roughly 835 km. NASA NSSDC OMNIWeb provides the IMP-8 hourly average solar wind data.

3. Method for inferring plasma sheet ion temperature, density, and pressure from ionospheric observations

The method for inferring the plasma sheet temperature, density, and pressure from the DMSP SSJ4 measurements has been described fully elsewhere [*Wing and Newell*, 1998; 2000; and Wing et al., 2005] and is briefly summarized here.

It has been known for more than two decades that energetic ions observed in the topside ionosphere are isotropic above a certain latitude [e.g., *Bernstein et al.*, 1974]. Likewise, an overwhelming number of in situ observations in the plasma sheet tailward of ~8–10 *RE* that indicate that plasma is nearly isotropic irrespective of activity levels [e. g., *Kistler et al*., 1992; *Spence et al*., 1989; *Huang and Frank*, 1994; *Sarris et al.*, 1981]. As a result, density, temperature, and pressure are conserved along the magnetic field line. The ions maintain their isotropy by pitch-angle scattering in the tail current sheet [*Lyons and Speiser,* 1982]. The physical mechanism is quite simple: ions cannot maintain their magnetic moments while traversing field lines that have a radius of curvature that is a significant fraction of their gyroradii [*Sergeev et al.,* 1993]. In the region where the curvature of the field line is small, the cross-tail current bends magnetic field lines enough to cause pitch-angle scattering whenever an ion crosses the current sheet [*Lyons and Speiser*, 1982; *Sergeev et al*., 1993]. Nearer to Earth (typically earthward of ~8–10 *RE*, although it varies with magnetic activity), the field line becomes more dipolar and the pitch-angle scattering ceases. As a result, the plasma becomes trapped, the particle precipitation drops drastically, and our method does not work in this region. This is the basis for the identification of the latitude of the equatorward isotropy boundary in the ionosphere (b2i) or equivalently the earthward boundary of the central plasma sheet (CPS) [*Newell et al*., 1996, 1998; *Sergeev et al*., 1993]. Because b2i (expressed in the magnetic latitude in degrees) has a local time variation, it is normalized to its midnight value.

The earthward boundary of the plasma sheet moves closer to the Earth, and the magnetotail magnetic field line becomes more stretched with the increasing magnetic activity. Hence, b2i decreases with increasing magnetic activity (see, for example, the plot of *Kp* versus b2i in Figure 1 of *Wing and Newell* [2003]). An important consequence of this result is that b2i can be used to indicate the stretching of the field lines and to improve the magnetic field model.

In fact, *Sergeev et al*. [1993] confirm this relationship by showing that there is a 0.9 correlation coefficient between the latitude of the ion isotropy boundary (or b2i) and the tail inclination angle measured in the same local time sector by GOES geosynchronous satellites. Therefore b2i can be used to modify and improve the ionosphere–magnetosphere tail mapping of the T89 magnetic field model [*Tsyganenko*, 1989]. The unmodified T89 model uses *Kp*, a 3-hour averaged index, as one of the input parameters, but the modified T89 model uses an additional input parameter, b2i, which is an instantaneous index. In the modified T89 model, the b2i is used as an index to modify the tail current slightly so that the tail field line stretching empirically agrees well with that of GOES observations (see Figure 7 of *Sergeev and Gvozdevsky* [1995]). The mapping accuracy from the ionosphere to the equatorial plane in the original T89 model has been investigated by *Pulkkinen and Tsyganenko* [1996]. They find that the mapping errors are generally small, <1 *RE* in the equatorial plane for $Kp < 3$ for magnetic latitude (mlat) <69° (in SM coordinate system). For mlat >69° (for the region further down the tail and closer to open field lines), they find that the error is <1 *RE* in the *x* direction and <3 *RE* in the *y* direction. With b2i, the modified T89 model provides an even more accurate and instantaneous field line tail mapping.

Electron acceleration events accelerate electrons downward and retard ions. These events have to be excluded from the data because they distort the plasma sheet particle spectra, resulting in distributions that do not represent those in the plasma sheet. An algorithm developed by *Newell et al*. [1996] to identify the electron acceleration events is used. Then, each individual ion spectrum that is not an electron acceleration event is fitted to three spectral forms: (1) one-component Maxwellian, (2) two-component Maxwellian, and (3) kappa (κ) distribution [e.g., *Vasyliunas*, 1971; *Christon et al*., 1988, 1989]. From these three fits, the best fit is selected according to reduced $\chi 2$ and $F\chi$ tests, which takes into account the number of free parameters

used [*Bevington*, 1969]. The spectrum is discarded if no fit is statistically valid. Unlike moment calculations, which are widely used, fitting the differential energy flux, $dj(E)/dE$, to a phase space density function takes into account ions outside the detector's energy range. The plasma sheet ions have been observed to have an energy range from a few eV up to a few hundred keV or higher [e.g., *Kistler et al*., 1992; *Christon et al*., 1988, 1989; *Lennartsson and Shelley*, 1986; *Meng et al*., 1981]. The density obtained using our method is higher than that obtained from the moment calculation.

In the 2D equatorial profiles, the average density, temperature, and pressure are calculated in 1 *RE* × 1 *RE* bins. Valid values are given only if there are at least 10 good points present in each bin. In addition, each spectrum is considered good only if there is another good spectrum (as determined by the fit criteria mentioned above) with similar distribution found within 4 sec (30 km in ionosphere).

In the present paper, the temperature reported for the κ distribution is the generalized temperature, which is given as follows. The κ distribution is given by

$$f_k(W) = n\left(\frac{m}{2\pi\kappa W_0}\right)^{\frac{3}{2}} \frac{\Gamma(\kappa+1)}{\Gamma\left(\kappa-\frac{1}{2}\right)}\left(1+\frac{W^*}{\kappa W_0}\right)^{-(\kappa+1)} \tag{1}$$

where n = density, m = mass, $W^* = \left(\sqrt{W}-\sqrt{W_s}\right)^2$, W = energy = 0.5 $mv2$, v = velocity, and Ws = shift energy [*Baumjohann and Treumann*, 1997]. *W0* is the particle energy peak of the distribution and can be related to the average thermal energy by

$$W_0 = k_B T\left(1-\frac{3}{2\kappa}\right) \tag{2}$$

Note that for κ >> 1, equation (2) reverts back to the simple Maxwellian case. Thus, the generalized temperature is

$$k_B T = \frac{2\kappa W_0}{2\kappa - 3} \quad (3)$$

The method does have limitations. One of the more significant ones is that because of the uncertainty in the ionosphere-magnetosphere mapping, the method is not suitable for studying microscale features of the plasma sheet, but it should be adequate for macroscale or global phenomena. However, previous studies have shown that the plasma sheet cooling and densification during periods of northward IMF are macroscale phenomena [*Stenuit et al*., 2002; *Øieroset et al*., 2005].

Extensive comparisons of the inferred plasma sheet density, temperature, and pressure with those obtained from in situ measurements [e.g., *Lennartsson and Shelley*, 1986; *Lennartsson*, 1992; *Baumjohann et al*., 1989; 1990; *Huang and Frank*, 1994; *Angelopoulos et al*., 1993; *Angelopoulos*, 1996; *Spence et al*., 1989] show fairly good agreement [*Wing and Newell*, 1998] with some caveats as discussed above and in *Wing and Newell* [2003; 1998].

4. The northward IMF plasma sheet density and temperature profiles

We applied the method described in section 3 to the DMSP data for the entire year of 1992. In this section, the statistical northward IMF plasma sheet profile was constructed by selecting the DMSP observations obtained when the simultaneous hourly averaged IMF is northward. Figure 1 shows the resulting northward IMF 2D ion density and temperature profiles on the equatorial plane [from Figure 4 in Wing et al., 2005]. In this study, all the observations are mapped to the equatorial plane and hence herein the plasma sheet refers to the central plasma sheet (CPS). Figure 1 affirms that the plasma sheet gets cold and dense during periods of northward IMF (for example, Figure 1 can be compared with the southward IMF ion density and profiles in *Wing and Newell* [2002]). As previously shown, in the inner plasma sheet region, around 8–10 *RE*, the plasma sheet is hotter in the dusk-midnight sector than in the

midnight-dawn sector [*Wing and Newell*, 1998; 2002]. This difference can be attributed to the gradient and curvature drift, which moves hotter ions duskward, as clearly demonstrated in some model calculations [*Spence and Kivelson*, 1993; *Wang et al*., 2001; 2002; 2003].

In addition to the dawn-dusk asymmetry in the inner edge of the plasma sheet, which results from the ion motion, there are other dawn-dusk asymmetries further down the tail in the flanks. As a start, Figure 1 shows that the density is higher along the dawn flank than along the dusk flank. The density peaks and temperature minima along the flanks have been previously identified as signatures of magnetosheath ion entry [e.g., *Wing and Newell*, 1998; 2002]. These signatures have been produced in the *Wang et al*. [2001; 2002; 2003] model and the Finite Width Magnetotail Convection (FWMC) model [*Spence and Kivelson*, 1993]. These models have two ion sources: (1) magnetosheath ions (cold), along the flank magnetopause and (2) nominal plasma sheet ions (hot), which originate further down the tail (tailward of the model boundary). In the models, the density peaks and temperature minima along the flanks are the results of the magnetosheath ion entry and the subsequent $\mathbf{E} \times \mathbf{B}$ earthward convection (the FWMC model has a magnetosheath ion source only on the dawn flank, and hence the model result only shows density peak and temperature minimum along the dawn flank).

As a result of the magnetosheath ion entry, plasma sheet ion distributions often have two components due to the mixing of the colder magnetosheath ions and hotter nominal plasma sheet ions, but in some regions, particularly along the dawn flank, many often appear to have only one component [*Fujimoto et al*., 1998; *Hasegawa et al*., 2003; 2004a; Wing et al., 2005]. Because the two-component Maxwellian fit in our study separates the distribution into hot and cold components, the properties of these two components can be investigated individually. Wing et al. [2005] studied both the hot and cold components and found that the cold component densities have maxima along both flanks, suggesting that the source and the entry points of the cold ions

lie along and/or near the magnetopause (see model calculations of *Wang et al*. [2001; 2002; 2003]; *Spence and Kivelson* [1993]). Moreover, the density peaks at both flanks in Figure 1, which shows the combined hot and cold components, can be attributed mostly to the cold component ions. In contrast, the hot component ion density profile does not have any peak along the flanks, suggesting that the source is not the adjacent LLBL or magnetosheath, although they may have entered at distant tail and then convect and heat up by the time they reach the mid-tail or near-Earth [Wing et al., 2005]. The temperatures and densities of the hot and cold components are displayed in Figure 2.

5. Plasma sheet specific entropy profiles

Using observations from in situ satellites, Borovsky examined the specific entropies of magnetosheath, LLBL, distant plasma sheet, mid-tail plasma sheet, and near-Earth plasma sheet. He found that the ions for the near-Earth, mid-tail, and near-Earth plasma sheets have more or less the same specific entropies. This can be discerned from Figure 3, which plots the ions in the log T – log n space. The figure shows that ions from the distant, mid-tail, and near-Earth lie on the same line (termed adiabat) albeit the scatter is large. In contrast, the magnetosheath ions have lower entropies than the plasma sheet entropies and have distinctly different adiabats from the plasma sheet ions, as shown in Figure 3. There are at least two important considerations for plasma sheet entry and transport (not specifically for northward IMF) based on this study. First the results are consistent with adiabatic earthward convection of plasma sheet material in the far tail. However, it should be noted that total entropy, S, is generally not conserved [Erickson and Wolf, 1980; Erickson, 1992; Garner et al., 2003; Kaufmann et al., 2004, Wing and Johnson, 2008]. Second, it is clear that the entropy of magnetosheath plasma; cold, dense plasma sheet material; and nominal plasma sheet material is significantly different and not adiabatically

connected. This finding suggests that whatever process leads to entry of cold, dense, material from the magnetosheath is nonadiabatic likely involving diffusion and heating processes, which will be discussed later.

For this study, we focus on northward IMF periods and consider the behavior of the combined (hot + cold) entropy as well as the entropy of the cold and hot components separately. We present profiles of the specific entropy, s, inferred from DMSP plasma sheet observations shown in Figure 1 assuming all particles have the same mass so that $s = P/\rho^{\gamma} \sim T/n^{\gamma-1}$. Figure 4a shows the entropy profile of the combined hot and cold ions. As discussed in section 4, during northward IMF, massive solar wind/magnetosheath ions enter the plasma sheet from both the dawn and dusk flanks. The solar wind entry increases the cold component ion population while lowering the temperature along the flanks [Figure 6 in Wing et al., 2005]. In terms of entropy, an important consequence of solar wind/magnetosheath entry is that it lowers the entropy at both flanks relative to the nominal plasma sheet material in the center of the plasma sheet, as shown in Figure 4a. This result can be understood by noticing that (1) solar wind/magnetosheath ions have significantly lower entropy than plasma sheet ions, as shown in Figure 3; and (2) solar wind/magnetosheath ion entry increases the cold (low entropy) ion population, by a factor of 2 of more [Wing et al., 2005].

In order to understand the role of the nominal plasma sheet and cold plasma during northward IMF conditions, it is also useful to treat each species individually. In a multi-fluid plasma each species would evolve according to its own equation of state conserving the entropy of that species if there is no heat exchange between species or other nonadiabatic processes such as precipitation or wave-particle interactions. The individual entropies would be conserved along drift paths if the evolution of the population were adiabatic.

Figure 4b shows the specific entropy profile for the hot component. The profile shows a dawn-dusk asymmetry with the dusk side having higher entropy than the dawn side. This would be consistent with the dawn-dusk heat flux carried by the gradient/curvature drift. The source of such ions is likely to be from the tail, which would explain why very few hot ions are found near the dawn flank (the hotter ions have drifted toward the dusk flank by curvature and gradient drift as they move earthward). Moreover, the gradient in the entropy increases closer to earth where curvature and gradient drift would be stronger relative to any convective motion.

The cold component entropy profile is shown in Figure 4c. Unlike the entropy profile for the hot component, the cold component profile does not exhibit much dawn-dusk asymmetry, apparently because curvature/gradient drift affects the cold ions much less than hot ions. Consequently, in the absence of nonadibatic processes, cold ions would tend to stay within the same flux tube volume during (earthward) convection and cold ions' specific entropies tend to be conserved in the convection path. Figure 4c shows that specific entropies are approximately conserved in the X (convection) direction. The conservation of entropy in the X direction can also be seen in the total (combined hot and cold) entropy profiles in Figure 4a, even though the hot components may not necessarily conserve specific entropies. This is because the total entropy profile is dominated by the cold ions. Wing et al. [2005] finds that cold component density can be more than twice as large as hot component density, depending on the locations and cold ion pressures can be comparable to hot ion pressures because of the increased density. This result is consistent with the results obtained with in situ observations as shown in Figure 3. The figure shows that points from the distant, mid-tail, and near-Earth plasma sheet tend to lie on the same adiabat albeit with a large scatter. The large scatter may be due to the curvature/gradient drift of the hotter ions and other non-adiabatic motions. It would be expected

that if the ions are separated by their energies their specific entropies might show less scatter along the convection path, which is not necessarily always in the X direction.

A more prominent feature in the cold ion entropy profile in Figure 4c is the specific entropy increases toward the center (midnight) meridian by a factor of five. The increase in entropy occurs gradually over a region around 10 RE on the dawn flank and is more gradual on the dusk flank. The increase in entropy is related to two features in the cold, dense plasma profile. First, the density decreases away from both of the flanks suggestive that the flanks are the source of the plasma. Second, there is heating of the plasma (mostly on the dawn flank that leads to a larger increase in entropy).

6. Discussion

Perhaps one of the more amazing features evident in the entropy profiles is that while the individual entropy for hot and cold plasma appear to have strong gradients (suggestive of the importance of diffusion and/or curvature and gradient drifts), the total entropy does appear to conserve fairly well in the X-direction. Consequently, it may be that MHD, which would lead to conservation of entropy in the X direction with a dawn-dusk convection electric field, could achieve reasonable results for plasma sheet evolution. However, the source population (from the tail) does appear to have a significant Y dependence, which presumably would result from nonadiabatic processes related to reconnection. This result suggests that the accuracy of MHD in describing tail transport may be related to how well it can describe the processes leading to the source population in the tail. On the other hand, it is apparent that a fluid approach based on adiabatic pressure evolution is not as useful to understand the behavior of the hot and cold component distributions where the entropies are clearly not conserved.

While it is fairly clear how the hot population could develop a heat flux in the duskward direction because of curvature and gradient drifts, it is not clear what mechanism(s) could transport the cold, dense ions to the center of the plasma sheet with an associated increase in entropy. Section 1 summarizes the three most commonly mentioned mechanisms for transporting ions from the magnetosheath to the plasma sheet, namely cusp reconnection in both hemispheres [Song and Russell, 1992], KHI [Otto and Fairfield, 2000], and KAW [e.g., Johnson and Cheng, 1997]. Any of these three mechanisms can transport the ions from the magnetosheath to the flanks of the plasma sheet. However, during northward IMF, cold dense ions have been observed not just at the flanks but also near the midnight meridian of the plasma sheet in studies using in situ as well as in DMSP data [e.g., Wing et al., 2005; 2006; Oieroset et al., 2005; Stenuit et al., 2002]. Another mechanism that may or may not be identical to the solar wind entry mechanism is needed to transport the cold ions further inward toward the midnight meridian.

One of the issues raised by the results of Borovsky [1998] is that the entropy of the cold, dense plasma is in general significantly larger than the magnetosheath entropy. The cusp reconnection model explains the cold, dense plasma as being captured by a field-line that has reconnected. It is useful to compare the specific entropy of the plasma in the reconnected flux tube with the specific entropy of sheath plasma assuming that they come from the same source. Birn [2006] showed with MHD and PIC simulations of a Harris sheet that reconnection is basically entropy conserving. Although the total entropy may change due to topology (change of flux tube volume) the specific entropy should be unmodified along most of the field line. For am MHD description of double cusp reconnection, as the field-line convects along the flank to the tail after reconnection, it might be expected that the entropy would be conserved leading to cooling of plasma as the density decreases due to an increase in flux tube volume. Such an adiabatic expansion is not consistent with observations of plasma heating in the cold, dense

population along the flanks [Wing et al., 2005], nor is it consistent with observations that show the entropy increases in the plasma sheet.

However, in considering the evolution of entropy for plasma that reconnects is important to recognize that there can be a discontinuous change in the second adiabatic (bounce motion) for particles on reconnected field lines. Conservation of entropy is closely tied to the bounce motion of particles which is analogous to a slowly moving piston in thermodynamics. In principle, particles on reconnected field lines would freely expand along the field line until they mirror. They would only gain or loose energy as they mirror in the changing field. Therefore, after reconnection there is a transient period where particles should expand freely along the field line carrying a heat flux until most of the particles begin to mirror. During this transient period the entropy would not be conserved (although the second adiabatic invariant would be conserved for individual particles). After the particles redistribute along the field line so that the heat flux reduces and the plasma reaches quasi-equilibrium after which the specific and total entropy would be conserved. In thermodynamics this process (reconnection) would be equivalent to removing a partition that would allow gas to fill a larger volume. Such expansion rather than being adiabatic is isothermal because particles do not gain or loose energy from a moving wall (piston). A rough estimate on entropy loss due to this process can be obtained by considering that the total plasma content fills the volume isothermally (this would be an upper bound if the flux tube subsequently expands).

In cusp reconnection the reconnected flux tube consists of a part that is of magnetosheath origin and the remainder of the flux tube is of magnetospheric origin (with much smaller density, but higher temperature). Let us consider only the change of entropy for the cold plasma captured on the sheath field line considering an isothermal expansion to fill the reconnected flux tube. Suppose that the flux tube volume of the magnetosheath portion of the field line is V_{sheath} and the

flux tube volume of the magnetospheric portion of the field line is V_{sphere}, then the total field line content of cold plasma is $N = n_{sheath} V_{sheath}$. After expansion the density is $N/(V_{sphere} + V_{sheath})$ so that $s_f/s_0 = (1 + V_{sphere} /V_{sheath})^{\gamma-1}$ and $\Delta s/s_0 \sim (\gamma-1) (V_{sphere} /V_{sheath})$ is the increase in entropy when the magnetospheric flux volume is much less than the captured volume. For double cusp reconnection, the captured sheath flux volume (where B is smaller and field line length is larger) should be much larger than the magnetospheric flux volume (where B is larger and field line length is shorter). Thus the change is small and double cusp reconnection by itself could not explain an observed entropy increase by a factor of 5 relative to the magnetosheath plasma. If cusp reconnection is responsible for the cold-dense plasma sheet it is most likely operating in conjunction with heating and diffusive processes that would lead to particle loss from the flux tube.

The Kelvin-Helmholtz instability has the potential to modify entropy along the boundary layer. While the MHD Kelvin-Helmholtz instability is entropy conserving, in the nonlinear stage of the instability the vortex structure can be on the order of the ion gyroradius where dissipative processes can lead to particle diffusion and heating through coupling to the kinetic Alfvén wave [Johnson and Cheng, 1997, 2001]. Moreover, in the nonlinear stage of the instability vortices can pinch off due to reconnection leading to flux tubes that contain magnetospheric and magnetosheath populations. Similar to the case of cusp reconnection, there will be a change of specific entropy of the cold population, s, given by $s_f/s_0 = (1 + V_{sphere} /V_{sheath})^{\gamma-1}$. However, unlike the cusp reconnection, it is more likely in this case that $V_{sphere} /V_{sheath}>1$ because only a small segment of total flux is actually detached magnetosheath plasma. Therefore a large increase on the order of 5 could be possible for the cold population as the cold population expands into the flux system attached to earth.

More importantly, there also can be a change of total entropy, S for the field line. Here we will consider the combined entropy consisting of both cold and hot particles, which at the time of reconnection were nearly in equilibrium (such that pressure is almost constant along the magnetic field). Suppose that prior to reconnection the total entropy per unit flux along the magnetosheath boundary is S_0 with volume V_0 and density n_0. If a flux volume V_{sheath} of sheath plasma with density n_{sheath} and pressure p_{sheath} reconnects to a portion of that field line with flux volume $(V_0 - V_1)$ and density n_{sphere} and pressure p_{sphere}, then the change in total entropy

$$\Delta S/S_0 = -(V_1/V_0) + (p2/p1)^{1/\gamma}(V_{sheath}/V_0).$$

Assuming that $V_1 \sim V_2$, then $\Delta S/S_0 \sim (V_{sheath}/V_0)((p_{sheath}/p_{sphere})^{1/\gamma} - 1)$. Because the magnetosheath particle pressure is smaller than the magnetospheric particle pressure in general, there will be a loss of total entropy. Reductions in total entropy can be significant because they can lead to interchange instability [Gold, 1959; Sonnerup, 1963; Hill, 1976] which can lead to transport of plasma flux into the inner magnetosphere. Therefore, such Kelvin-Helmholtz reconnection would lead to a reduction in total entropy (a bubble) which could then move earthward due to interchange motion convecting the plasma earthward into the plasma sheet [e.g., Birn, 2006].

Large-amplitude ULF waves that are frequently observed at the magnetopause boundary [Anderson et al., 1982; Tsurutani et al., 1982; Rezeau et al., 1986; Labelle et al., 1988; Rezeau et al., 1989; Engebretson et al., 1991a, Engebretson et al., 1991b; L in et al., 1991; Takahashi et al., 1991; Rezeau et al., 1993; Song et al., 1993, Song et al., 1993; Song et a1., 1993; Anderson et al., 1994; Song et al., 1994; Phan et al., 1994; Phan et al., 1996a; Phan et al., 1996b] may also be important for transport. One of the more common spectral features at the magnetopause boundary is the sharp transition in wave polarization from compressional, e.g., due to foreshock waves of the quasi-parallel bow shock, to transverse waves from the magnetosheath to the boundary layers [Johnson and Cheng:1997; Johnson and Cheng, 2001; Chaston et al., 2008]. It

has been suggested that the mode conversion from compressional to Alfvén modes provides a source of Alfven waves in the magnetosphere [Johnson and Cheng:1997; Johnson and Cheng, 2001; Chaston et al., 2008]. Multipoint measurements have verified that the dispersion of the broadband waves is consistent with kinetic Alfven waves [Chaston et al., 2007; 2008]. Such waves have been seen in conjunction with reconnection events and Kelvin-Helmholtz waves which may also be sources of free energy to drive the waves. The presence of kinetic Alfvén waves leads to heating and transport of plasma consistent with (a) global requirements for the plasma entry rate and (b) observed transverse ion heating [Johnson and Cheng, 2001, Chaston et al., 2008]. Kinetic Alfvén waves also provide a natural explanation for the observed dawn-dusk asymmetry in plasma entry during northward IMF [Hasegawa et al., 2003; Wing et al., 2005] because they result from mode conversion of compressional foreshock waves, which typically bathe the dawn flank for typical Parker spiral configuration. This asymmetry could be related to the asymmetry in the cold plasma entropy profiles.

That kinetic Alfvén waves can lead to plasma transport and heating can be seen in simple test particle calculations illustrated in Figure 6. A bath of ten kinetic Alfvén waves with amplitude $\delta E \sim 4$mV/m is prescribed consistent with a linear dispersion relation with random frequency and $k_\perp \rho_i \sim 1$ with random orientation in the plane perpendicular to the magnetic field. Cold particles are inserted at a constant rate at X=0. In the absence of waves these cold particles would remain at X=0. However, in the presence of the waves, the particles are able to diffuse across the magnetic field as described in Johnson and Cheng [1997]. In addition the amplitudes are large enough that ion orbits can become chaotic leading to ion heating described in Johnson et al., [2001]. Particles that reach the right hand boundary of the simulation at $X=7\rho_i$ are removed. As time progresses, the particle density profile develops a constant gradient between the source and the boundary consistent with a diffusive process. The diffusion coefficient can be

obtained by considering the ratio of the flux of particles leaving the domain to the slope of the density profile. We have also plotted the entropy profile, which shows that the specific entropy increases as the result of plasma diffusion (reducing density) and plasma heating, which increases temperature. The influx of cold particles on magnetospheric field lines would also decrease the total entropy as for the Kelvin-Helmholtz instability leading to the possibility of interchange motion that could convect the plasma away from the diffusive boundary region into the center of the plasma sheet.

An important issue seen in the statistical results is that specific entropy increases toward the center of the plasma sheet. If interchange instabilities occur, they normally would transport flux tubes with lower total entropy earthward. However, plasma in those flux tubes should conserve entropy as fixed by the value at the boundary, and therefore it is an interesting question why the entropy would increase toward the plasma sheet. One possibility is that the diffusion is very large in the center of the plasma sheet as estimated by Borovsky [2003]. However, for diffusion coefficients the order of $D = 10^9$-10^{10} m^2/s as commonly found near the magnetosheath boundary the diffusion time to bring plasma to the center of the plasma sheet is the order of $t \sim L^2/D > 100$hrs. Therefore, it is likely that a convective process may be important for moving the material into the center of the plasma sheet.

It is interesting to consider whether entropy gradients that arise in the boundary layer due to diffusion or plasma mixing could, in principle, be responsible for the large-scale entropy gradients across the flanks. Convective processes (such as interchange) could lead to gradients in the entropy even in regions where entropy is conserved. To see this, consider a simple diffusion equation

$$\partial n / \partial t + v_c \partial n / \partial x = D \partial^2 n / \partial x^2 - \nu n$$

in a domain consisting of a source population at X=0, a diffusion region, with constant diffusion coefficient D and no convection, of width Δ adjacent to a convection region with constant convection velocity v and little/no diffusion. The purpose of this calculation is not to provide a rigorous model for plasma sheet convection, but to simply show that gradients in the entropy profile in the convection region may result from dynamics in the diffusion region. In Figure 5 we illustrate the solution as a function of time with $D=10^9 m^2/s$, X in RE, and v_c=1Re/hr as an average convection velocity. We may also prescribe a realistic plasma loss in the diffusion region that might result from convection along the magnetopause boundary, which would prevent the diffusive process from eventually filling the diffusion region. For this calculation, we arbitrarily choose ν=0.2hr. Initially there is no cold plasma in the domain. As time progresses particles diffuse across the diffusion region. After 1 hour, the plasma enters the convection region. As time progresses, the density increases on the inner edge of the diffusion region. Assuming that the temperature at the boundary reaches a fixed maximum value (consistent with KAW heating, which is bounded by the wave amplitude [Johnson et al., 2001]), the entropy is fixed by the increasing density. Because the entropy in a plasma element is conserved during the convection a profile of increasing entropy develops in the cold population that convects in the X direction. The gradient forms because plasma that convects away from the convection boundary earlier has higher entropy than plasma that convects away later. Consequently, diffusive processes can, in fact, produce entropy gradients in the plasma sheet far away from the boundary because the source of the plasma is varying in time. Slow or intermittent convective processes can therefore be responsible for the entropy gradients observed in the center of the plasma sheet even if entropy is dynamically conserved in that region.

Summary

In this paper we have discussed the specific entropy of the plasma sheet for northward IMF. We found that the specific entropy of the plasma is nearly constant in the X direction, but has strong gradients across the plasma sheet with minima near the flank boundaries. By examining the hot and cold populations separately, we found that the entropy profiles for each species is quite different. The hot population entropy profile indicates an azimuthal heat flux across the plasma sheet consistent with curvature and gradient drift. Not surprisingly, this feature is not seen in the cold population which is not as affected by magnetic field gradients. On the other hand, the cold population shows a significant gradient in entropy from the flanks to the center of the plasma sheet. As an observational constraint, the specific entropy of the cold, dense, plasma suggests that cusp reconnection by itself is not adequate to explain the increase of specific entropy in the cold, dense plasma sheet material because entropy is more or less conserved in the global reconnection process. However, kinetic Alfvén waves are often observed in conjunction with reconnection and may provide heating and plasma losses from reconnected flux tubes. On the other hand, localized reconnection in Kelvin-Helmholtz vortices may provide a significant increase in the specific entropy because the cold material originates in only a small flux tube volume and will spread out to populate the entire field line. Similarly, kinetic Alfvén waves lead to plasma diffusion and heating consistent with the observed plasma profiles. Given the fact that these changes in entropy occur in the boundary layer, we also considered whether the plasma sheet entropy profiles could also be determined by the plasma behavior in the boundary. In fact, we have shown that the time dependent behavior of plasma profiles at the inner edge of a diffusion region could be mapped to spatial variation in entropy in the plasma sheet by a convective process. These maps provide an important constraint for theoretical models of particle entry and transport in the plasma sheet.

Acknowledgments. Gordon Wilson has been helpful in our acquiring DMSP SSJ4 data, as has the World Data Center in Boulder, Colorado. Simon Wing gratefully acknowledges the support of NSF Grants ATM-0703445, ATM-0802715, and ATM-0538513; and NASA Grant NNX06AB87G. Jay R. Johnson acknowledges support from NASA grants (NNH04AB23I, NNH04AA73I, NNG06GE96G, NNX06AB87G and NNH07AF37I), and NSF grants (ATM0411392 and ATM0614012, add our NSF grant), and DOE contract DE-AC02-76CH03073.

References

Anderson, R. R., C. C. Harvey, M. M. Hoppe, and B. T. Tsurutani 1982), Plasma wave near the magnetopause, J. Geophys. Res. , 87, 2087.

Angelopoulos, V., W. Baumjohann, C. F. Kennel, F. V. Coroniti, M. G. Kivelson, R. Pellat, R. J. Walker, H. Lu¨hr, and G. Paschmann (1992), Bursty bulk flows in the inner central plasma sheet, J. Geophys. Res., 97,4027–4039.

Angelopoulos, V., et al. (1993), Characteristics of ion flow in the quiet state of the inner plasma sheet, Geophys. Res. Lett., 20, 1711 – 1714.

Ashour-Abdalla, M., et al. (1998), Determination of particle sources for a Geotail distribution function observed on May 23, 1995, in Geospace Mass and Energy Flow, edited by J. L. Horwitz et al., pp. 297– 312, AGU, Washington, D.C.

Bernstein, W., B. Hultqvist, and H. Borg (1974), Some implications of low altitude observations of isotropic precipitation of ring current protons beyond the plasmapause, *Planet. Space Sci*., 22, 767.

Baumjohann, W., and G. Paschmann (1989), Determination of the polytropic index in the plasma sheet, Geophys. Res. Lett., 16, 295– 298.

Baumjohann, W., R. Schodel, and R. Nakamura, Bursts of fast magnetotail flux transport (2002), Adv. Space. Sci., 30, 2241-2246.

Baumjohann, W., G. Paschmann, and C. A. Cattell (1989), Average plasma properties in the central plasma sheet, *J. Geophys. Res*., *94*, 6597–6606.

Baumjohann, W., The near-Earth plasma sheet: An AMPTE?IRM perspective (1993), Spa Sci Rev, 64, 141-163, 1993.

Birn J., M. Hesse, and K. Schindler (2006), On the role of entropy conservation and entropy loss governing substorm phases, Int. Conf. Substorms-8, 19-24.

Birn J., M. Hesse, and K. Schindler (2006), Entropy conservation in simulations of magnetic reconnection, *Phys. Plasmas, 13*, 092117, DOI:10.1063/1.2349440.

Borovsky, J. E., M. F. Thomsen, and R. C. Elphic (1998), The driving of the plasma sheet by the solar wind, J. Geophys. Res., 103, 17,617–17,639.

Borovsky, J. E., M. F. Thomsen, R. C. Elphic, T. E. Cayton, and D. J. McComas (1998b), The transport of plasma sheet material from the distant tail to geosynchronous orbit, J. Geophys. Res., 103, A9, 20,297-20,331.

Borovsky, J. E., and H. O. Funsten, MHD turbulence in the Earth's plasma sheet: Dynamics, dissipation, and driving, *J. Geophys. Res.*, *108*(A7), 1284, doi:10.1029/2002JA009625, 2003.

Chen, C. X., and R. A. Wolf (1993), Interpretation of high-speed flows in the plasma sheet, J. Geophys. Res., 98, 21,409-21,419.

Chaston, C., et al. (2008), Turbulent heating and cross-field transport near the magnetopause from THEMIS, Geophys. Res. Lett., 35, 17.

Chaston, C. C., M. Wilber, F. S. Mozer, M. Fujimoto, M. L. Goldstein, M. Acuna, H. Reme, and A. Fazakerley (2007), Mode conversion and anomalous transport in Kelvin-Helmholtz vortices and kinetic Alfv{\'e}n waves at the Earth's magnetopause, Phys. Rev. Lett., 99, 175,004.

Engebretson, M. J., J. L. Cahil, Jr., R. L. Arnoldy, B. J. Anderson, T. J. Rosenberg, D. L. Carpenter, U. S. Inan, and R. H. Eather (1991a), The role of the ionosphere in coupling upstream ULF wave power into the dayside magnetosphere, J. Geophys. Res., 96, 1527.

Engebretson, M. J., N. Lin, W. Baumjohann, H. Luehr, B. J. Anderson, L. J. Zanetti, T. A. Potemra, R. L. McPherron, and M. G. Kivelson (1991b), A comparison of ULF fluctuations in the solar wind, magnetosheath, and dayside magnetosphere: 1. Magnetosheath morphology, J. Geophys. Res., 96, 3441.

Erickson, G. M., and R. A. Wolf (1980), Is steady convection possible in the Earth's magnetotail, Geophys. Res. Lett., 7, 897.

Erickson, G. M. (1992), A quasi-static magnetospheric convection model in two dimensions, J. Geophys. Res., 97, 6505-6522.

Friedel, R. H. W., H. Korth, M. G. Henderson, and M. F. Thomsen (2001), Plasma sheet access to the inner magnetosphere, *J. Geophys. Res*., *106*, 5845-5858.

Fujimoto, M., T. Terasawa, T. Mukai, Y. Saito, T. Yamamoto, and S. Kokubun (1998), Plasma entry from the flanks of the near-Earth magnetotail: Geotail observations, *J. Geophys. Res*., *103*, 4391-4408.

Garner, T. W., R. A. Wolf, R. W. Spiro, M. F. Thomsen, and H. Korth (2003), Pressure balance inconsistency exhibited in a statistical model of magnetospheric plasma, J. Geophys. Res., 108(A8), 1331, doi:10.1029/2003JA009877.

Gjerloev, J. W., R. A. Hoffman, J. B. Sigwarth, L. A. Frank (2007), Statistical description of the bulge-type auroral substorm in the far ultraviolet, *J.Geophys.Res*., in press.

Goertz, C. K., and W. Baumjohann (1991), On the thermodynamics of the plasma sheet, *J. Geophys. Res.*, *96*, 20,991-20,998.

Gold, T., Motions in the magnetosphere of the earth, *J. Geophys. Res*., *64*, 1219, 1959.

Gombosi, T. I., and A. F. Nagy (1989), Time-dependent modeling of field-aligned current-generated ion transients in the polar wind, *J. Geophys. Res*., *94*, 359-369.

Hasegawa, H., M. Fujimoto, K. Maezawa, Y. Saito, and T. Mukai (2003), Geotail observations of the dayside outer boundary region, J. Geophys. Res., 108, SMP 9-1 to SMP 9-16.

Hill, T. W., Interchange stability of a rapidly rotating magnetosphere, *Planet. Space Sci., 24*, 1151, 1976.

Hori, T., K. Maezawa, Y. Saito, and T. Mukai (2000), Average profile of ion flow and convection electric field in near-Earth plasma sheet, Geophys. Res. Lett., 27, 1623–1626.

Huang, C. Y., and L. A. Frank (1994), A statistical survey of the central plasma sheet, *J. Geophys. Res*., 99, 83-95.

Johnson, J. R., and C. Z. Cheng (1997), Kinetic Alfv{\'e}n waves and plasma transport at the magnetopause, Geophys. Res. Lett., 24, 1423 – 1426.

Johnson, J. R., and C. Z. Cheng (2001), Stochastic ion heating at the magnetopause due to kinetic Alfv{\'e}n waves, Geophys. Res. Lett., 28, 4421- 4424.

Johnson, J. R., C. Z. Cheng, and P. Song (2001), Signatures of Mode Conversion and Kinetic Alfv{\'e}n Waves at the Magnetopause, Geophys. Res. Lett., 28, 227 - 230.

Huang, C. Y., C. K. Goertz, L. A. Frank, and G. Rostoker (1989), Observational determination of the adiabatic index in the quiet time plasma sheet, Geophys. Res. Lett., 16, 563– 566.

Kamide, Y., and S. Kokubun (1996), Two-component auroral electrojet: Importance for substorm studies, *J.Geophys.Res*., *101*, 13.027.

Kaufmann, R. L., W. R. Paterson, and L. A. Frank (2004), Pressure, volume, density relationships in the plasma sheet, J. Geophys. Res., 109, A08204, doi:10.1029/2003JA010317.

Kaufmann, R. L., and W. R. Paterson 2006), Magnetic flux and particle transport in the plasma sheet, J. Geophys. Res., 111, A10214, doi:10.1029/2006JA011734.

Kennel, C. F. (1969), Consequences of a mangetospheric plasma, Rev. Geophys., 7, 379.

Kistler, L. M., E. Mobius, W. Baumjohann, G. Paschmann, and D. C. Hamilton (1992), Pressure changes in the plasma sheet during substorm injections, *J. Geophys. Res*., *97*, 2973-2983.

Kivelson, M. G., and H. E. Spence (1988), On the possibility of quasistatic convection in the quiet magnetotail, Geophys. Res., Lett., 15, 1541-1544.

Korth, H., M. F. Thomsen, J. E. Borovsky, and D. J. McComas (1999), Plasma sheet access to geosynchronous orbit, *J. Geophys. Res., 104*, 25,047-25,061.

Labelle, J., and R. A. Treumann (1988), Plasma waves at the dayside magnetopause, Space. Sci. Rev., 47, 175 - 202.

Lin, N., M. J. Engebretson, R. L. McPherron, M.~G. Kivelson, W. Baumjohann, H. Luehr, T. A. Potemra, B. J. Anderson, and L. J. Zanetti (1991), A comparison of ULF fluctuations in the solar wind, magnetosheath, and dayside magnetosphere. II. Field and plasma conditions in the magnetosheath, J. Geophys. Res., 96, 3455 - 3464.

Lui, A. T. Y. (1991), Extended consideration of a synthesis model for magnetospheric substorms, in *Magnetospheric Substorms*, pp. 43-60, *Geophys. Monog.*, *64*, edited by J. R. Kan, T. A. Potemra, S. Kokubun, and T. Ijima, AGU, Washington D.C.,

Lyons, L. R., and T. W. Speiser (1982), Evidence for current sheet acceleration in the geomagnetic tail, J. Geophys. Res., 87, 2276-2286.

Lyons, L. R., C.-P. Wang, T. Nagai, T. Mukai, Y. Saito, and J. C. Samson (2003a), Substorm inner plasma sheet particle reduction, *J. Geophys. Res*., 108(A12), 1426, doi:10.1029/2003JA010177.

Lyons, L. R., C.-P. Wang, and T. Nagai (2003b), Substorm onset by plasma sheet divergence, *J. Geophys. Res*., 108(A12), 1427, doi:10.1029/2003JA010178.

McPherron, R. L., C. T. Russell, and M. P. Aubry (1973), Satellite studies of magnetospheric substorms on August 15, 1968, 9, Phenomenological model for substorms, *J. Geophys. Res*., 78, 3131.

Nagai, T., M. Fujimoto, Y. Saito, S. Machida, T. Terasawa, R. Nakamura, T. Yamamoto, T. Mukai, A. Nishida, and S. kokubun (1998), Structure and dynamics if nagnetic reconnection for substorm onsets with Geotail observations, J. Geophys. Res., 103, 4419-4440.

Opgenoorth, H. J., M. A. L. Persson, T. I. Pulkkinen, and R. J. Pellinen (1994), Recovery phase of magnetospheric substorms and its association with morning-sector aurora, *J. Geophys. Res*., *99*, 4115-4129.

Paterson, W. R., L. A. Frank, S. Kokubun, and T. Yamamoto (1998), Geotail survey of ion flow in the plasma sheet: Observations between 10 and 50 RE, J. Geophys. Res., 103, 11,811 – 11,825.

Phan, T.-D., G. Paschmann, W. Baumjohann, N. Sckopke, and H. Luehr (1994), The magnetosheath region adjacent to the dayside magnetopause: AMPTE/IRM observations, J. Geophys. Res., 99, 121 - 141.

Phan, T.-D., G. Paschmann, and B. U. O. Sonnerup (1996a), Low-latitude dayside magnetopause and boundary layer for high magnetic shear 2. Occurrence of magnetic reconnection, J. Geophys. Res., 101, 7817-7828.

Phan, T.~D., et~al. (1996b), The subsolar magnetosheath and magnetopause for high solar wind ram pressure: WIND observations, Geophys. Res. Lett., 23, 1279 - 1282.

Pontius, D. H., and R. A. Wolf (1990), Transient flux tubes in the terrestrial magnetosphere, Geophys. Res. Lett., 17, 49-52.

Pulkkinen, T. I., and N. A. Tsyganenko (1996), Testing the accuracy of magnetospheric model field line mapping, *J. Geophys. Res., 101*, 27,431-27,442.

Rezeau, L., S. Perraut, and A. Roux (1986), Electromagnetic fluctuations in the vicinity of the magnetopause, Geophys. Res. Lett., 13, 1093 - 1096.

Rezeau, L., A. Morane, S. Perraut, A. Roux, and R. Schmidt (1989), Characterization of Alfvénic fluctuations in the magnetopause boundary layer, J. Geophys. Res., 94, 101 - 110.

Rezeau, L., A. Roux, and C. T. Russell (1993), Characterization of small-scale structures at the magnetopause from ISEE measurements}, J. Geophys. Res., 98, 179 - 186.

Sergeev, V. A., M. Malikov, and K. Mursula (1993), Testing the isotropic boundary algorithm method to evaluate the magnetic field configuration in the tail, *J. Geophys. Res*., 98, 7609-7620.

Sergeev, V. A., V. Angelopoulos, J. T. Gosling, C. A. Cattell, and C. T. Russell (1996), Detection of localized, plasma-depleted flux tubes or bubbles in the midtail plasma sheet, J. Geophys. Res., 101, 10,817– 10,826.

Song, P., C. T. Russell, and C. Y. Huang (1993a), Wave properties near the subsolar magnetopause - Pc 1 waves in the sheath transition layer, J. Geophys. Res., 98, 5907 - 5923.

Song, P., et al. (1993b), Structure and properties of the subsolar magnetopause for northward interplanetary magnetic field - Multiple-instrument particle observations, J. Geophys. Res., 98, 11,319.

Song, P., C. T. Russell, and S. P. Gary (1994), Identification of low-frequency fluctuations in the terrestrial magnetosheath, J. Geophys. Res., 99, 6011 - 6025.

Spence, H. E., and M. G. Kivelson (1993), Contributions of the low-latitude boundary layer to the finite width magnetotail convection model, *J. Geophys. Res*., *98*, 15,487-15,496.

Spence, H. E., M. G. Kivelson, R. J. Walker, and D. J. McComas (1989), Magnetospheric plasma pressures in the midnight meridian: Observations from 2.5 to 35 *RE*, *J. Geophys. Res.*, *94*, 5264–5272.

Stenuit, H., M. Fujimoto, S. A. Fuselier, J.-A. Sauvaud, S. Wing, A. Fedorov, E. Budnik, S. P. Savin, K. J. Trattner, V. Angelopoulos, J. Bonnel, T. D. Phan, T. Mukai, and A. Pedersen (2002), Multi-spacecraft study on the dynamics of the dusk-flank magnetosphere under northward IMF: January 10-11, 1997, *J. Geophys. Res.*, *107*(A10), 1333, doi:10.1029/2002JA9009246.

Takahashi, K., D. G. Sibeck, P. T. Newell, and H. E. Spence (1991), ULF waves in the low-latitude boundary layer and their relationship to magnetospheric pulsations - A multisatellite observation, J. Geophys. Res., 96, 9503 - 9519.

Terasawa, T. et al. (1997), Solar wind control of density and temperature in the near-Earth plasma sheet: WIND/GEOTAIL collaboration, *Geophys. Res. Lett.*, *24*, 935-938.

Tsurutani, B. T., and R. M. Thorne (1982), Diffusion processes in the magnetopause boundary layer, Geophys. Res. Lett., 9,1247--1250.

Tsyganenko, N. A. (1982), On the convective mechanism for formation of the plasma sheet in the magnetospheric tail, Planet Space Sci., 30, 1007-1012.

Tsyganenko, N. A. (1989), A magnetospheric magnetic field model with a warped tail current sheet, *Planet Space Sci.*, *37*, 5-20.

Tung, Y.-K., C. W. Carlson, J. P. McFadden, D. M. Klumpar, G. K. Parks, W. J. Peria, and K. Liou (2001), Auroral polar cap boundary ion conic outflow observed on FAST, J. Geophys. Res., 106, 3603-3614.

Usadi, A., R. A. Wolf, M. Heinemann, and W. Horton (1996), Does chaos alter the ensemble averaged drift equation?, J. Geophys. Res., 101, 15,491.

Wang, C. P., L. R. Lyons, M. W. Chen, and R. A. Wolf (2001), Modeling the quiet time inner plasma sheet protons, J. Geophys. Res., 106, 6161.

Wang, C.-P., L. R. Lyons, M. W. Chen, and F. R. Toffoletto (2004), Modeling the transition of the inner plasma sheet from weak to enchanced convection, *J. Geophys. Res., 109*, A12202, doi:10.1029/2004JA010591.

Wang, C.-P., L. R. Lyons, J. M. Weygand, T. Nagai, and R. W. McEntire (2006), Equatorial distributions of the plasma sheet ions, their electric and magnetic fields under different interplanetary magnetic field Bz conditions, J. Geophys. Res., 111, A04215, doi:10.1029/2005JA011545.

Wang, C.-P., L. R. Lyons, T. Nagai, J. M. Weygand, and R. W. McEntire (2007), Sources, transport, and distributions of plasma sheet ions and electrons and dependence on interplanetary parameters under northward interplanetary magnetic field, J. Geophys. Res., 112, A10224, doi:10.1029/2007JA012522.

Wilson, G. R., D. M. Ober, G. A. germany, and E. J. Lund (2004), Nightside auroral zone and polar cap ion outflow as a function of substorm size and phase, *J. Geophys. Res*., *109*, A02206, doi:10.1029/2003JA009835.

Wing, S., and P. T. Newell (1998), Central plasma sheet ion properties as inferred from ionospheric observations, *J. Geophys. Res*., *103*, 6785-6800.

Wing, S., and P. T. Newell (2000), Quiet time plasma sheet ion pressure contribution to Birkeland currents, *J. Geophys. Res*., *105*, 7793-7802.

Wing, S., D. G. Sibeck, M. Wiltberger, and H. Singer (2002), Geosynchronous magnetic field temporal response to the solar wind and IMF variations, *J. Geophys. Res*., 107(A8), doi:10.1029/2001JA009156.

Wing, S., and Patrick T. Newell (2002), 2D plasma sheet density profile for northward and southward IMF, *Geophys. Res. Lett*., 29(9), 10.1029/2001GL013950.

Wing, S., J. R. Johnson, P. T. Newell, and C.-I. Meng (2005), Dawn-dusk asymmetry in the northward IMF plasma sheet, *J. Geophys. Res*., *110*, A08205, doi:10.1029/2005JA011086.

Winglee, R. M., W. Lewis, and G. Lu (2005), Mapping of the heavy ion outflows as seen by IMAGE and multifluid global modeling for the 17 April 2002 storm, *J. Geophys. Res.*, *110*, A12S24, doi:10.1029/2004JA010909.

Wolf, R. A., V. Kumar, F. R. Toffoletto, G. M. Erickson, A. M. Savoie, C. X. Chen, and C. L. Lemon (2006), Estimating local plasma sheet $PV^{5/3}$ from single-spacecraft measurements, *J. Geophys. Res*., *111*, A12218, doi:10.1029/2006JA012010.

Wolf, R. A. (1983), The quasi-static (slow-flow) region of the magnetosphere, in Solar-Terrestrial Physics, edited by R. L. Carovillano and J. M. Forbes, p. 303, D. Reidel, Hingham, Mass, 1983.

Figure Caption

Figure 1. 2D equatorial profiles of plasma sheet ion (a) density and (b) temperature for northward IMF orientation. Each point is averaged over $1 \times 1\ R_E^2$ regions. Some regions are left blank either because of insufficient data points or because plasma is anisotropic (in the region closer to the Earth). (from Wing et al., 2005).

Figure 2. . (a) Density and (b) temperature profiles of the cold component of the two-component Maxwellian distribution of the plasma sheet ions. Note that the dawn-dusk asymmetry in the temperature profile, with the dawn flank ions having higher temperatures than the dusk flank ions. Note that the temperature scale is an order of magnitude lower than that used in other temperature profiles shown in the present paper. (c) density and (d) temperature profiles of the hot component of the two component Maxwellian distribution of the plasma sheet ions.

Figure 3. Entropy density of plasma sheet, LLBL, and magnetosheath ions in the n – T semi log space. The ions in the distant, mid-tail, and near-Earth plasma sheet tend to have the same adiabats, indicated by the diagonal lines with $\gamma = 5/3$ (from Joseph Borovsky, GEM presentation 2005).

Figure 4. Plasma sheet specific entropy profiles for (a) combined hot and cold components, (b) hot component, and (c) cold component. The hot component profiles shows a dawn-dusk gradient while the cold component profile shows s approximately conserved in the X direction and a gradient toward the midnight meridian.

Figure 5. Density, temperature, and specific entropy $\log_{10}(p/\rho^{\gamma})$ profiles in a direction across the magnetic field based on particle motion in a background magnetic field with a superposition of ten linear kinetic Alfvén wave solutions (averaged over ten realizations of the system). Cold particles are introduced at X=0 with zero velocity at a constant rate. As time progresses, the population diffuses away from the source toward the boundary. Particles are removed when their displacement from the source is seven ion gyroradii. The rate of particles exiting the domain is given by dn/dt in the fourth panel. As time progresses, the density profile develops constant slope from which we obtain a diffusion coefficient $D=2x10^{9}m^{2}/s$ for an electric field amplitude of 4mV/m (roughly a few nT for Alfvén waves) as is typical of magnetopause fluctuations. Heating of plasma occurs due to nonlinear wave particle resonance [Johnson and Cheng, 2001]. The diffusion of plasma across field lines combined with heating can lead to a change in specific entropy by a factor of 5

Figure 6. Development of the density profile for a convective process that is fed by a diffusive boundary layer. Profiles are plotted at 1 hour intervals from 1 to 10 hours (density increases in time from the initial profile of n(0,x)=0). As time progresses, density diffuses from a source at X=0 across a diffusive region of width D and is then convected further to larger X. This simple calculation illustrates how the time development of a density/entropy profile at the edge of a diffusive boundary layer could be mapped to a spatial profile of entropy in the plasma sheet. Such a profile may result from a combination of diffusion due to Kelvin-Helmholtz vortices or kinetic Alfvén waves at the boundary and interchange motion that transports plasma earthward.

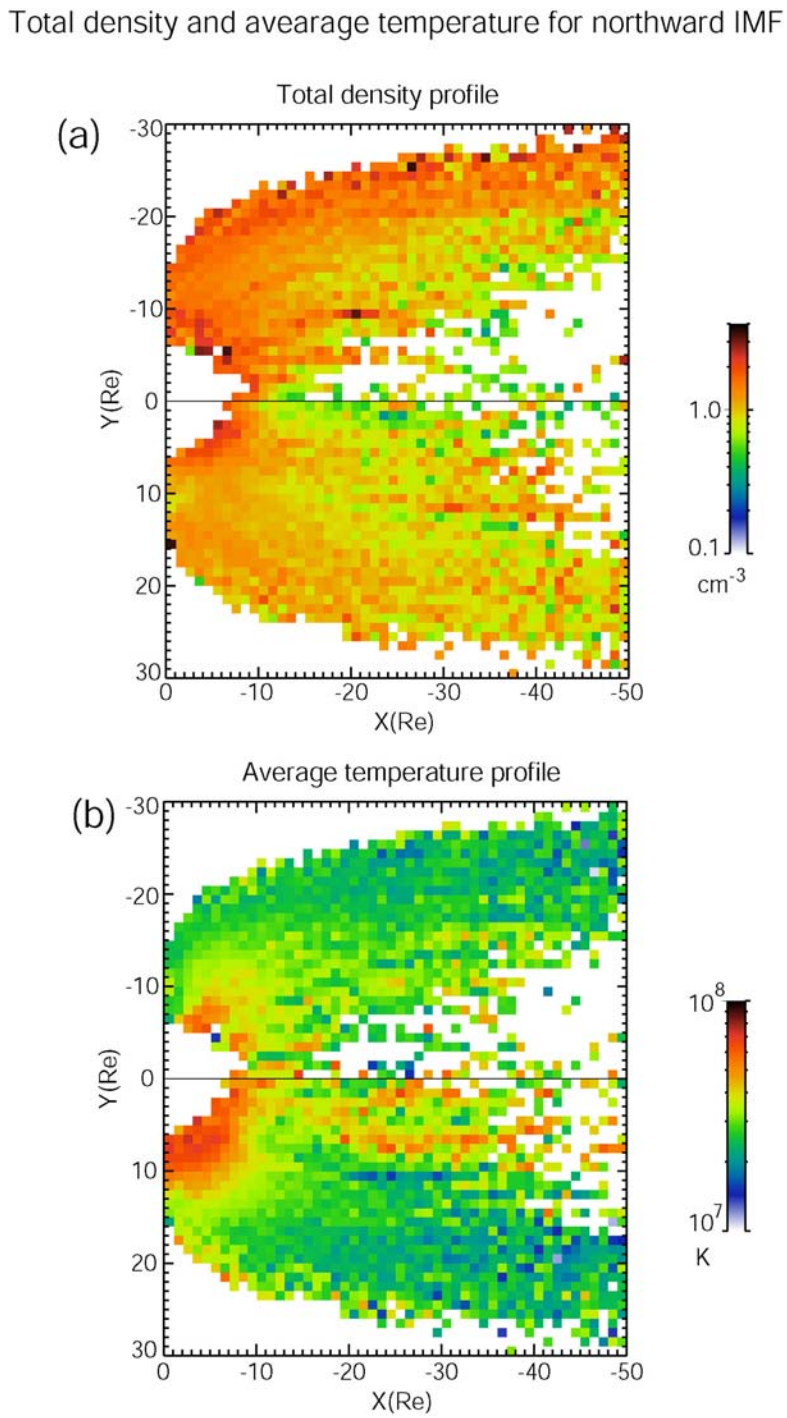
Total density and avearage temperature for northward IMF
Total density profile
(a)
Y(Re)
X(Re)
1.0
0.1
cm-3
Average temperature profile
(b)
Y(Re)
X(Re)
10^8
10^7
K

Figure 1

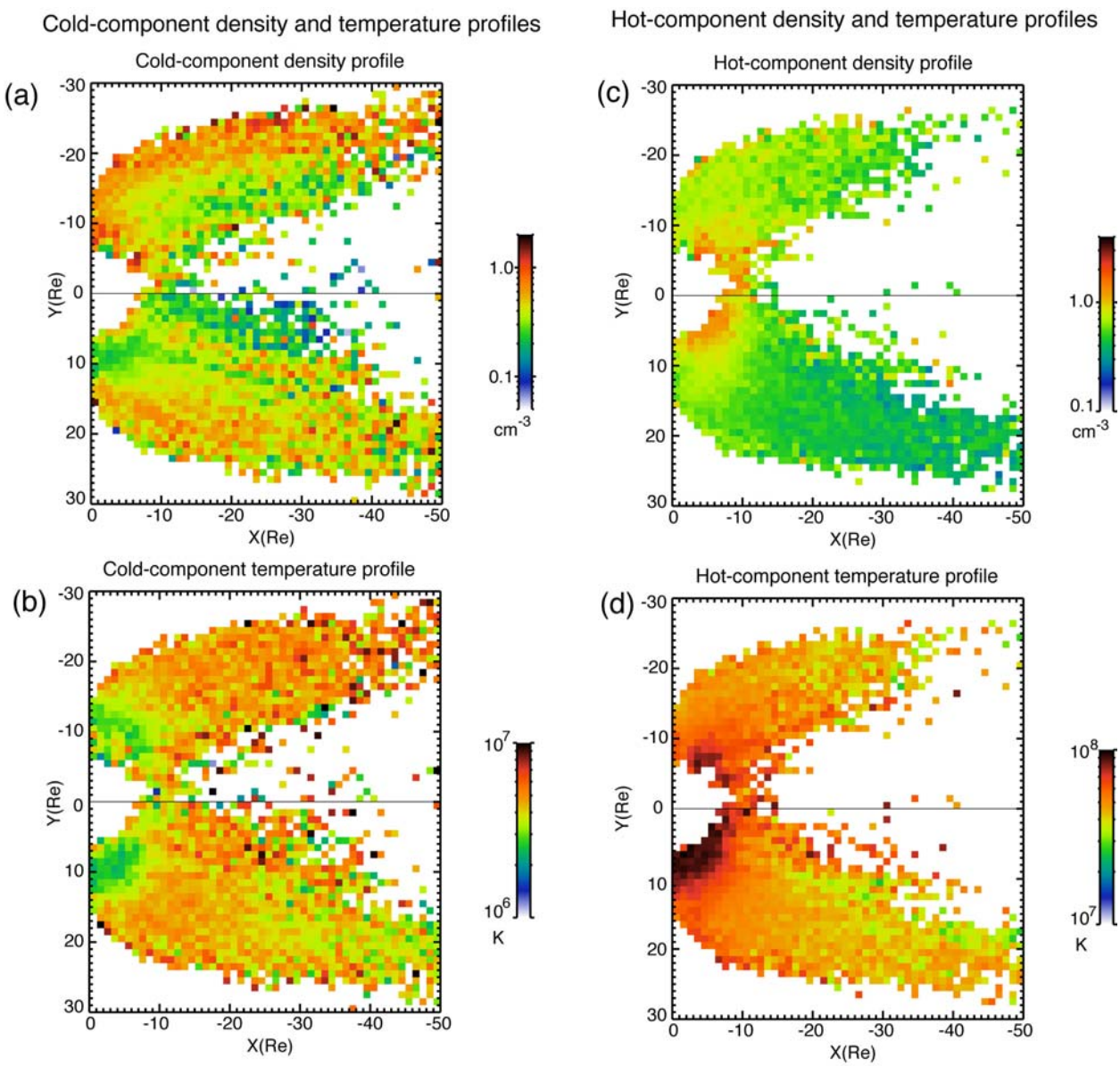
Cold-component density and temperature profiles
Hot-component density and temperature profiles
Cold-component density profile
Hot-component density profile
Cold-component temperature profile
Hot-component temperature profile
(a)
(b)
(c)
(d)
Y(Re)
X(Re)
1.0
0.1
cm-3
10^7
10^6
10^8
K

Figure 2.

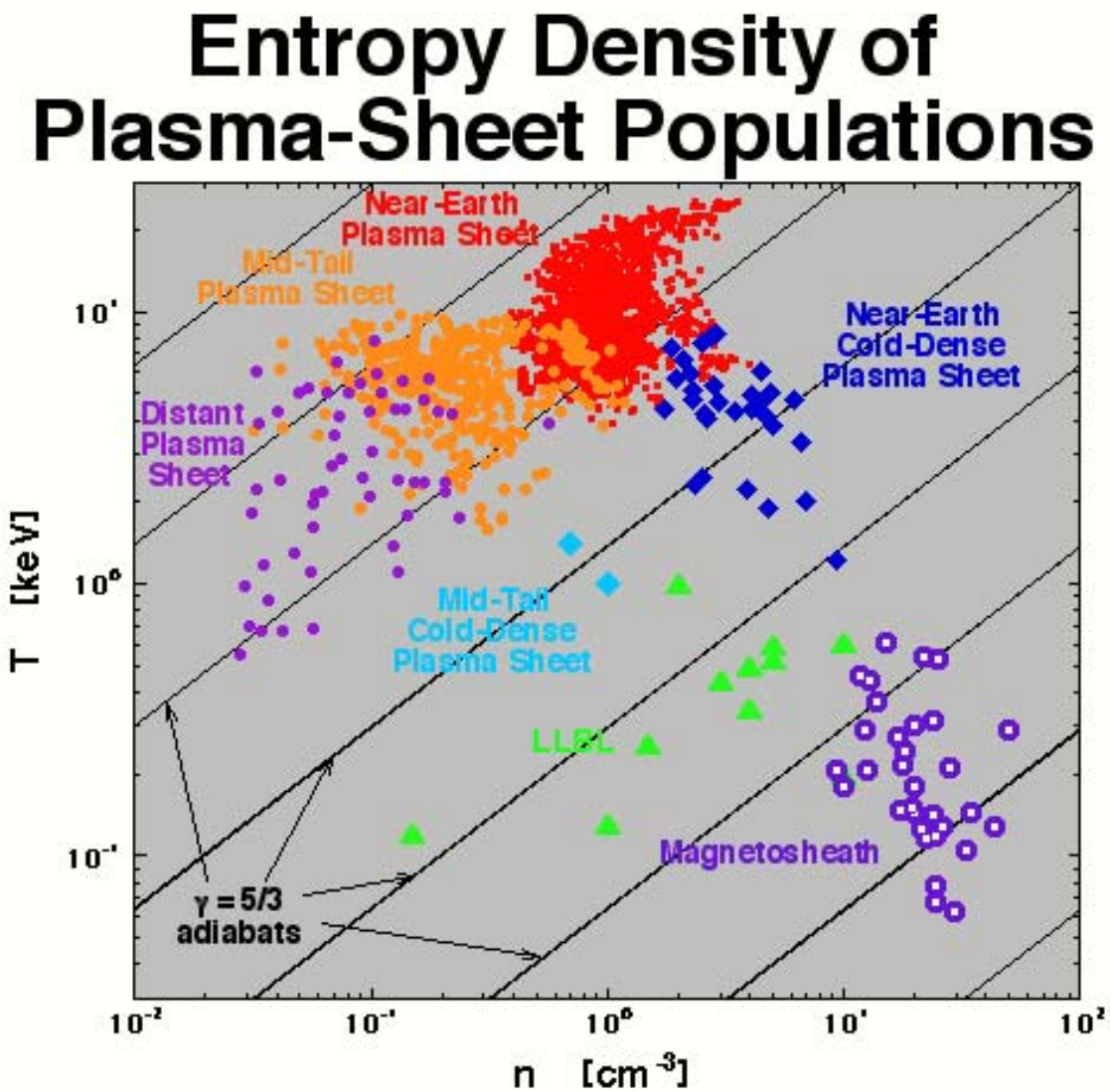
Entropy Density of
Plasma-Sheet Populations
Near-Earth
Plasma Sheet
Mid-Tail
Plasma Sheet
Near-Earth
Cold-Dense
Plasma Sheet
Distant
Plasma
Sheet
Mid-Tail
Cold-Dense
Plasma Sheet
LLBL
Magnetosheath
γ = 5/3
adiabats
T [keV]
n [cm⁻³]

Figure 3.

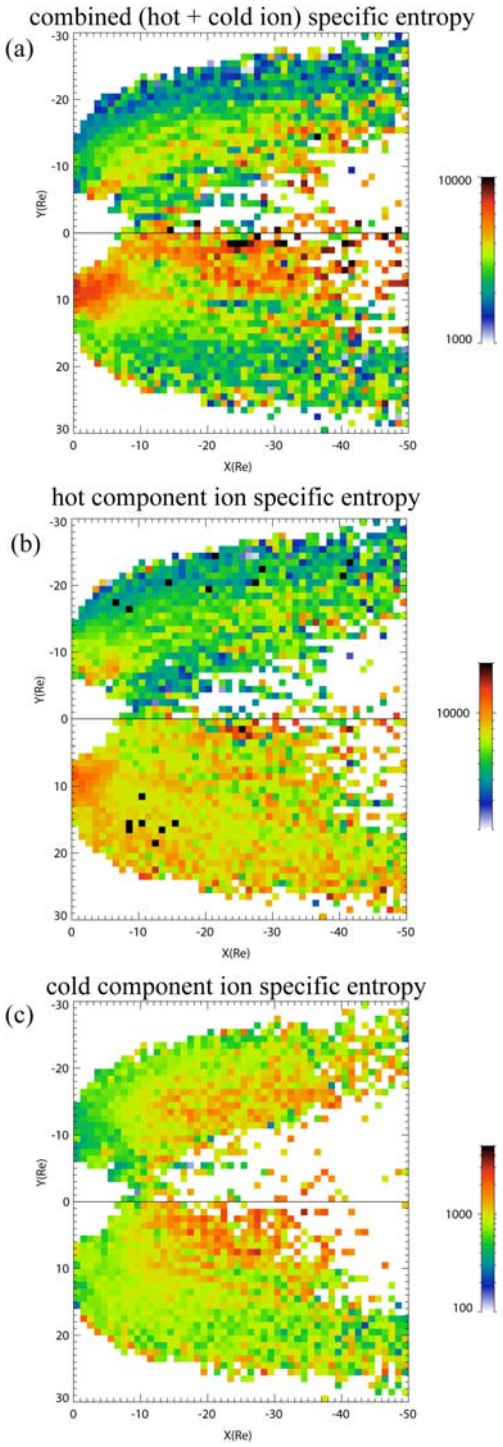
combined (hot + cold ion) specific entropy
(a)
Y(Re)
X(Re)
10000
1000
hot component ion specific entropy
(b)
Y(Re)
X(Re)
10000
cold component ion specific entropy
(c)
Y(Re)
X(Re)
1000
100

Figure 4

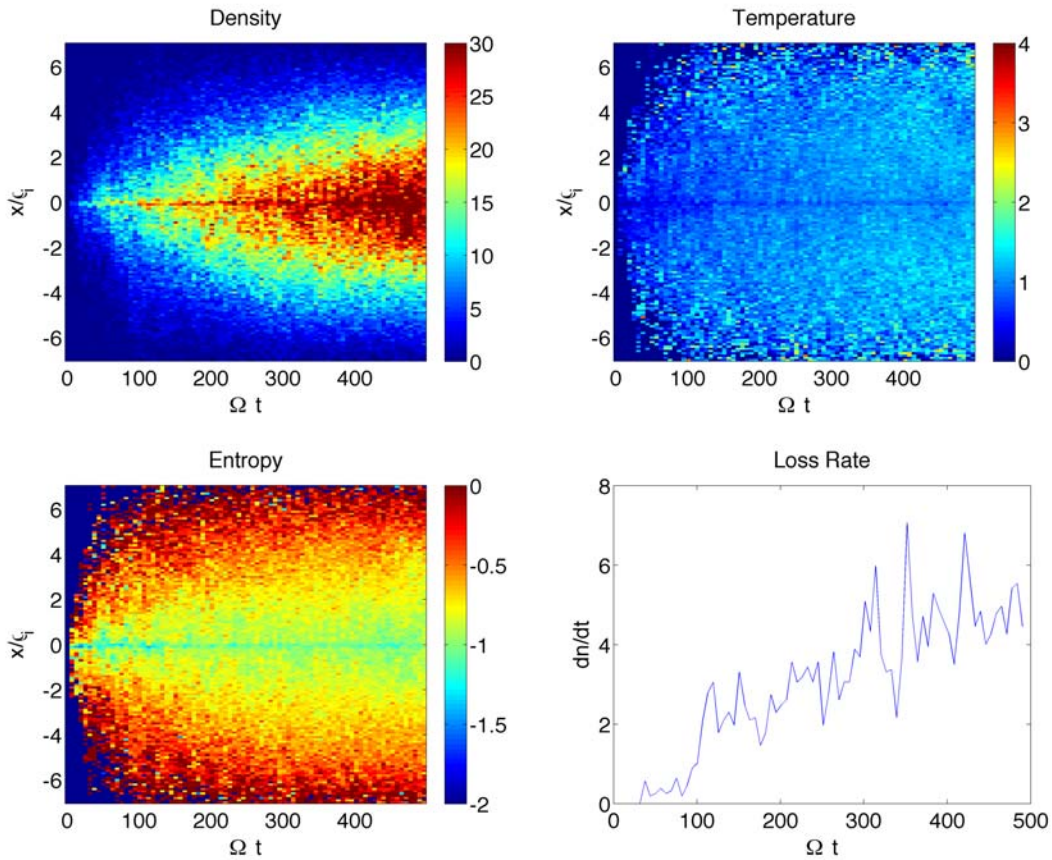

Figure 5.

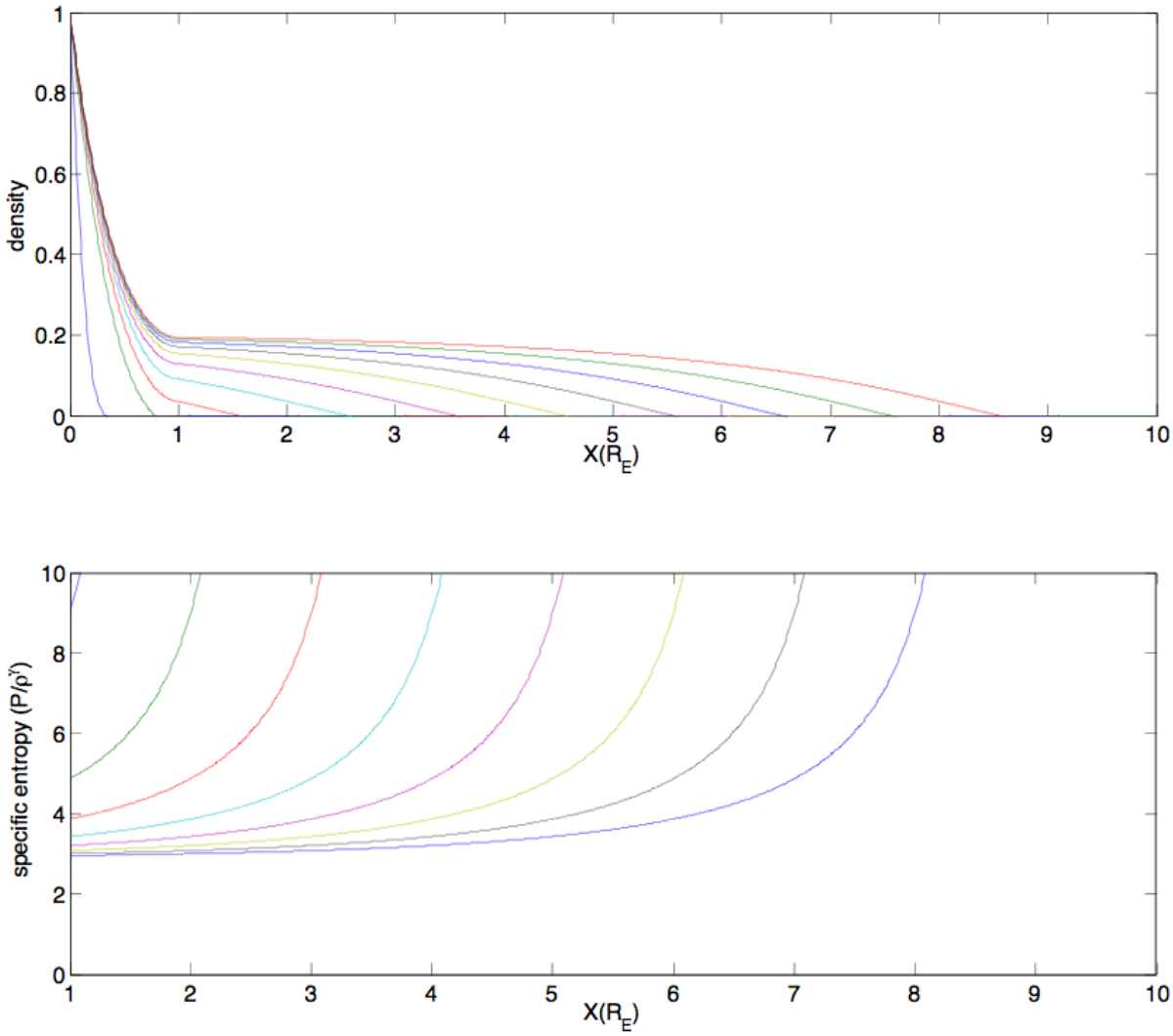

Figure 6.